



Published in final edited form as:

*Mucosal Immunol.* 2022 February ; 15(2): 244–256. doi:10.1038/s41385-021-00474-8.

## Disruption of monocyte-macrophage differentiation and trafficking by a heme analog during active inflammation

Rachel E. M. Schaefer<sup>1,3,4</sup>, Rosemary C. Callahan<sup>1,3,4</sup>, Shaikh M. Atif<sup>2</sup>, David J. Orlicky<sup>5</sup>, Ian M. Cartwright<sup>1,3,4</sup>, Andrew P. Fontenot<sup>2</sup>, Sean P. Colgan<sup>1,3,4</sup>, Joseph C. Onyiah<sup>1,3,4,#</sup>

<sup>1</sup>Division of Gastroenterology and Hepatology, University of Colorado School of Medicine, Aurora, CO

<sup>2</sup>Division of Allergy, Asthma and Clinical Immunology, University of Colorado School of Medicine, Aurora, CO

<sup>3</sup>Department of Medicine, University of Colorado School of Medicine, Aurora, CO

<sup>4</sup>Rocky Mountain Regional Veterans Affairs Medical Center, Aurora, CO

<sup>5</sup>Department of Pathology, University of Colorado School of Medicine, Aurora, CO.

### Abstract

Heme metabolism is a key regulator of inflammatory responses. Cobalt protoporphyrin IX (CoPP) is a heme analog and mimic that potently activates the NRF2/heme oxygenase-1 (HO-1) pathway, especially in monocytes and macrophages. We investigated the influence of CoPP on inflammatory responses using a murine model of colitis. Surprisingly, conditional deletion of myeloid HO-1 did not impact the colonic inflammatory response or the protective influence of CoPP in the setting of dextran sodium sulphate-induced colitis. Rather, we reveal that CoPP elicits a contradictory shift in blood myeloid populations relative to the colon during active intestinal inflammation. Major population changes include markedly diminished trafficking of CCR2<sup>+</sup>Ly6C<sup>hi</sup> monocytes to the inflamed colon, despite significant mobilization of this population into circulation. This resulted in significantly diminished colonic expansion of monocyte-derived macrophages and inflammatory cytokine expression. These findings were linked with significant induction of systemic CCL2 leading to a disrupted CCL2 chemoattractant gradient towards

---

Users may view, print, copy, and download text and data-mine the content in such documents, for the purposes of academic research, subject always to the full Conditions of use:[http://www.nature.com/authors/editorial\\_policies/license.html#terms](http://www.nature.com/authors/editorial_policies/license.html#terms)

# Corresponding author: Joseph C. Onyiah, M.D., University of Colorado School of Medicine, Rocky Mountain Regional VA Medical Center, 12700 East 19th Ave. MS B-146, Aurora, CO 80045, joseph.onyiah@cuanschutz.edu.

Author contributions

R.E.M.S.: Investigation, methodology, formal analysis, validation, writing. R.C.C.: Investigation, methodology, validation. S.M.A.: Conceptualization, investigation, methodology, editing. D.J.O.: Formal analysis (histo/pathologic scoring), validation. I.M.C.: Investigation, methodology. A.P.F. Resources, editing. S.P.C.: Conceptualization, funding acquisition, resources, supervision, editing. J.C.O.: Conceptualization, investigation, methodology, formal analysis, funding acquisition, resources, supervision, writing.

Conflict of Interest

The authors declare no competing financial interests.

Supplemental material

Fig. S1 shows full clinical scoring for a 7-day WT DSS experiment where mice were given vehicle vs CoPP. Fig. S2 examines anti-inflammatory differentiation of in vitro macrophages in response to CoPP. Fig. S3 evaluates the influences of myeloid *Hmox1* expression on BMM and murine colitis phenotypes. Fig. S4 examines colonic and blood myeloid populations in colitic *Hmox1*<sup>fl/fl</sup>/LysMcre mice comparing shifts in CoPP vs vehicle treated groups. Fig. S5 defines chemokine gradients produced by expression of CXCL1, CXCL2 and CCL11 in the colon and serum in a colitis experiment.

the colon and concentration-dependent suppression of circulating monocyte CCR2 expression. Administration of CoPP also induced macrophage differentiation toward a Marco<sup>hi</sup>Hmox1<sup>hi</sup> anti-inflammatory erythrophagocytic phenotype, contributing to an overall decreased inflammatory profile. Such findings redefine protective influences of heme metabolism during inflammation, and highlight previously unreported immunosuppressive mechanisms of endogenous CCL2 induction.

### Summary:

A heme analog and mimic triggers an anti-inflammatory CCL2 gradient in a model of colitis, resulting in contradictory suppressed trafficking of monocytes to the colon relative to the systemic circulation, as well as anti-inflammatory erythrophagocytic macrophage differentiation, independent of myeloid HO-1.

### Keywords

CCL2; CCR2; CoPP; colitis; cobalt protoporphyrin; innate immunity

---

### Introduction

Heme, otherwise known as iron(II) protoporphyrin IX, is a critical component of oxygen carrying hemoglobin. It is also a potent modifier of inflammatory responses partly through its regulation of the nuclear factor erythroid 2-related factor 2 (NFE2L2/NRF2) / heme oxygenase-1 (HO-1) pathway (1, 2). HO-1 is responsible for the metabolism of heme into carbon monoxide, iron and biliverdin. There are several analogs of heme with alternative metal atoms (metalloporphyrins) which have both inhibitory and activating influence on the NRF2/HO-1 pathway (3, 4). Heme is composed of a protoporphyrin IX ring system with a central complexed iron atom while the backbone of the heme analog CoPP is also a protoporphyrin IX ring, substituted with a central cobalt atom. Like heme, cobalt(II) protoporphyrin IX can reversibly bind oxygen (at much lower affinity) and is similarly metabolized by HO-1 (5–7). Unlike heme, the analog cobalt(III) protoporphyrin IX (CoPP/Co-heme) is not metabolized by HO-1 and therefore acts as a more potent and sustained activator of the NRF2/HO-1 pathway (4, 6, 8). HO-1 induction has been shown to be protective in a number of inflammatory disease models, including colitis (9–12). HO-1 influences inflammatory cytokine production, is anti-apoptotic and has antioxidative properties partly through removal of heme and partly through its metabolic products (9, 11). In acute and chronic intestinal inflammatory models, the protective influence of CoPP has been associated with the activity of monocyte/macrophage HO-1 (11, 13, 14). CoPP-induced HO-1, and its metabolic product carbon monoxide, have been linked with improved macrophage bacterial killing and decreased inflammatory cytokine expression. However, recent work has shown that CoPP can effectively mobilize myeloid cells to the circulation in the absence of inflammation and independent of NRF2/HO-1 (15). The influence of this myeloid mobilization on the protective impact of CoPP in inflammatory disease has not been examined. In light of this, we sought to clarify mechanisms responsible for the protective influence of CoPP in active inflammation using a murine colitis model.

In this study we examined anti-inflammatory mechanisms of CoPP in dextran sodium sulphate (DSS) induced colitis, a model of intestinal inflammation (16, 17). Oral exposure to DSS damages the intestinal epithelium leading to bacterial invasion and activation of the innate immune system (16–18). Previous work has shown that CCR2<sup>+</sup>Ly6C<sup>hi</sup> inflammatory monocytes are recruited to the colonic mucosa in the setting of DSS injury and differentiate into inflammatory effector and antigen presenting cells (19, 20). Ablation of these recruited monocytes ameliorates colitis (19). Similarly, recruited monocytes are a significant source of pro-inflammatory cytokines including IL-1 $\beta$ , TNF, IL-12 and IL-6 (19, 21–24). We found that CoPP treatment resulted in dual protective mechanisms in colitis. Namely, we reveal that CoPP inhibits trafficking of CCR2<sup>+</sup>Ly6C<sup>hi</sup> monocytes to the colon, secondary to disruption of the normal chemoattractive CCL2 gradient, culminating in marked suppression of monocyte CCR2 expression by its CCL2 ligand. This was associated with contradictory shifts in myeloid populations between the circulation and colon. Moreover, CoPP exposure led to the development of recently characterized anti-inflammatory erythrophagocytic macrophages in the colon, expressing high levels of HO-1 and MARCO mRNA (25). These findings unveil a distinctive CCL2 gradient driven anti-inflammatory response resulting in altered monocyte trafficking, differentiation and expansion.

## Results and discussion:

### Cobalt protoporphyrin protects against development of intestinal inflammation

To examine the protective influence of CoPP on intestinal inflammation we examined the response in DSS colitis. Exposure of WT mice to a course of oral DSS led to weight loss, diarrhea and hematochezia, summarized in a disease activity index (DAI) score, which typically peaks with DSS exposure at 5 days (Fig. 1A). IP administration of CoPP to WT mice during the course of DSS significantly decreased clinical manifestations of intestinal inflammation as well as histological measures of inflammation (Fig. 1B–C). Analysis of whole colon protein expression at day 5, the peak of DSS induced injury, using a mouse exploratory proteomics panel (Olink) revealed significant differences in protein expression patterns between mice that received and did not receive CoPP (Fig. 1D–E). This includes key cytokines such as TNF, IL-1 $\beta$ , CSF2, IL-10 and CXCL9 (Fig. 1F).

### Colonic transcriptome profile reveals anti-inflammatory mechanisms of CoPP

To clarify the colonic response to CoPP exposure, we performed RNA-seq analysis on whole colon tissue. We used healthy non-colitic WT mice that received water and were given CoPP or vehicle IP. Figure 2A shows a heat map representing significant colonic differential gene expression results. As expected, we observed elevated log<sub>2</sub> fold change expression of *Hmox1* (4.17; adj.  $p = 1.07 \times 10^{-11}$ ) in the CoPP exposed mice relative to vehicle. It is notable that, the most highly induced gene was *Marco* (7.80; adj.  $p = 2.92 \times 10^{-08}$ ), which is typically expressed by lung alveolar and splenic marginal zone macrophages (26–29). These findings were validated using qPCR of whole colon tissue (Fig. 2B). While *Marco* expression has not previously been described in colonic myeloid populations, recent work has shown that *Marco* mRNA is expressed in a population of liver F4/80<sup>+</sup> macrophages (including Kupffer cells) in the setting of hemolytic stress and NRF2 activation (25). These liver macrophages are described as Marco<sup>hi</sup>Hmox<sup>hi</sup>MHC class II<sup>lo</sup> erythrophagocytes and

have a distinct anti-inflammatory and anti-oxidant phenotype. In vitro macrophages exposed to heme developed a similar phenotype with a discrete gene signature separate from the well-known M1 (IFN- $\gamma$ /LPS-polarized) and M2 (IL-4-polarized) macrophages (25). Using immunohistochemistry, we found strong expression of HO-1 in healthy WT mouse colon in response to CoPP (Fig. 2C). We also found co-expression of F4/80 and HO-1 after CoPP exposure (Fig 2D) suggesting that F4/80<sup>+</sup> macrophages are the main source of HO-1. To further validate this finding, we used fluorescence-activated cell sorting (FACS) to isolate CD11b<sup>+</sup>CX3CR1<sup>+</sup>CD64<sup>+</sup>MHCII<sup>+</sup>Ly6C<sup>-</sup> macrophages from WT mice two days after treatment with CoPP or vehicle (Fig. S2A) (30, 31). We found that macrophages from CoPP treated mice exhibited lower surface expression of MHC class II, similar to the previously described erythrophagocytic macrophages in the liver. We then recovered mRNA from the macrophages to assess expression patterns, which further validated our RNA-seq findings. By qPCR we observed a NRF2 associated mRNA expression pattern comparable to the recently described erythrophagocytic liver macrophage phenotype (increased *Hmox1*, *Marco*), with similarity to splenic erythrophagocytic red pulp macrophages that express *Spic* (Fig. 2F) (25, 32). Moreover, when we treated these macrophages ex-vivo with LPS we noted a similar inhibition of LPS induced inflammatory gene expression in these CoPP exposed intestinal macrophages (Fig. 2G) (25). We examined the response to CoPP in vitro using M-CSF differentiated WT bone marrow-derived macrophages (BMMs). Pretreatment, >85% of the cells were CD11b<sup>+</sup>CX3CR1<sup>+</sup>F4/80<sup>+</sup>CD64<sup>+</sup> (Fig. S2B). We treated these BMMs with CoPP and after 48h, we observed significant surface expression of MARCO in response to CoPP treatment, more than LPS, a positive control (Fig. S2B) (26). These M-CSF differentiated BMMs also expressed other erythrophagocytic genes in response to CoPP (Fig. S2C). However, as previously reported, the induction of inflammatory genes in BMMs in response to LPS was much more robust than intestinal macrophages (33), while CoPP again led to lower levels of inflammatory gene expression relative to vehicle controls (Fig. S2D).

### Protective influence of cobalt protoporphyrin is independent of myeloid HO-1

To examine the importance of HO-1 to the development of intestinal inflammation in DSS colitis, we bred C57BL/6 *Hmox1*<sup>fl/fl</sup> mice with LysMcre mice to produce myeloid specific HO-1 deficient mice (*Hmox1*<sup>fl/fl</sup>/LysMcre). The expression of HO-1 is high in the monocyte-macrophage lineage given their role in clearance of aged or damaged erythrocytes, especially in the spleen and liver (34, 35). Myeloid HO-1 has been shown to regulate innate immune responses in murine models of inflammation and efficient deletion of HO-1 in macrophages in this setting has been previously described (36, 37). M-CSF cultured bone marrow-derived macrophages (BMMs) were derived from our *Hmox1*<sup>fl/fl</sup>/LysMcre mice and *Hmox1*<sup>fl/fl</sup> controls, then *Hmox1* mRNA expression was examined by qPCR; it was decreased in the *Hmox1*<sup>fl/fl</sup>/LysMcre BMMs compared to controls (85–95%). After differentiation of BMMs into M1 macrophages, we observed that the *Hmox1*<sup>fl/fl</sup>/LysMcre BMMs manifested a more pro-inflammatory phenotype in response to LPS. We observed markedly increased mRNA expression of *Il1 $\beta$*  (9.5 fold), *Nos2* (7.6 fold), *Tnf* (1.6 fold) and *Ccl2* (3 fold) compared to controls (Fig. S3A), confirming the anti-inflammatory role of HO-1 in macrophages (37). Given the increased inflammatory response with the loss of HO-1 expression, we expected that *Hmox1*<sup>fl/fl</sup>/LysMcre mice would develop more

severe colonic inflammation than controls in response to DSS. Surprisingly, we found no significant differences in measures of disease activity compared to controls (Fig. 3A). Moreover, *Hmox1*<sup>fl/fl</sup>/LysMcre mice that received CoPP showed significant improvement in DAI scores compared to vehicle treated *Hmox1*<sup>fl/fl</sup>/LysMcre mice, similar to the protection seen in WT mice (Fig. 3A and S3B–C). These results suggest that myeloid HO-1 does not regulate the response to acute DSS colitis including in the setting of CoPP treatment. Given the unexpected findings we examined *Hmox1* expression in intestinal macrophages from our *Hmox1*<sup>fl/fl</sup> and *Hmox1*<sup>fl/fl</sup>/LysMcre mice. We isolated intestinal macrophages (CD11b<sup>+</sup>CX3CR1<sup>+</sup>CD64<sup>+</sup>MHCII<sup>+</sup>Ly6C<sup>-</sup>) using FACS (Fig. S2A). We saw a significant decrease in *Hmox1* expression in our intestinal macrophages (~94%) from our *Hmox1*<sup>fl/fl</sup>/LysMcre mice compared to *Hmox1*<sup>fl/fl</sup> controls (Fig. 3B). This suggests efficient Cre recombinase activity in our target population and supports the observation that the protective benefit of CoPP in these mice is not dependent on intestinal macrophage *Hmox1* expression. An examination of relative populations of inflammatory monocytes, transitional monocytes (Ly6C<sup>+</sup>CCR2<sup>+</sup>MHCII<sup>+</sup>) and macrophages (Fig. S3C) in the *Hmox1*<sup>fl/fl</sup> and *Hmox1*<sup>fl/fl</sup>/LysMcre mice did not show any differences. When macrophages were isolated at the peak of DSS injury, we did not observe differences in select inflammatory cytokines in the macrophages from the *Hmox1*<sup>fl/fl</sup>/LysMcre mice, unlike what was observed with in vitro M-CSF cultured macrophages exposed to LPS (Fig. 3C). This suggests that macrophage HO-1 alone is not critical in the more complex colonic inflammatory response to DSS injury. In contrast, when intestinal macrophages were isolated from at the peak of DSS injury in WT mice, there was significantly less *Il1β* and *Il12b* expression in CoPP treated mice compared to vehicle controls (Fig. 3D) confirming prior ex-vivo findings that CoPP leads to anti-inflammatory differentiation of intestinal macrophages. Interestingly, at this specific timepoint *Tnf* expression was not different.

### Protective influence of CoPP is associated with contradictory shifts in myeloid populations

We examined the influence of CoPP on the colonic gene expression profile in active colitis. RNA-seq analysis of whole colon tissue in the setting of DSS injury demonstrated significant differences in gene expression in CoPP treated mice compared to controls (Fig. 4A). Similar to our findings in non-colitic mice, we observed upregulated log2 fold change gene expression of *Marco* (2.54; adj. p < .05) and *Hmox1* (2.68; adj. p = 9.16×10<sup>-12</sup>) in colitic mice exposed to CoPP (Fig. 4A). This is consistent with differentiation of erythrophagocytic macrophages in the setting of inflammation. We also observed a decrease in the expression of *Tnf*, *Il1β* and *Cxcl2* in CoPP treated mice, consistent with observed decreased inflammation in these mice (Fig. 4A). Interestingly, a gene ontology analysis suggested there were differences in leukocyte migration within the overall regulation of the immune response (Fig. 4B). CoPP has recently been demonstrated to mobilize myeloid cells into the bloodstream in a G-CSF dependent manner in mice (15). We therefore examined the influence of CoPP on leukocyte mobilization during active intestinal inflammation using our colitis model (Fig. 4C). Total and relative populations of blood leukocytes were characterized using flow cytometry in healthy mice and at the height of DSS-induced injury (Fig. 4D). We confirmed that there was a marked increase in myeloid mobilization to the bloodstream in CoPP treated mice compared to controls (Fig. 4E). This finding was also

observed in colitic mice that received CoPP, where we observed a significant increase in blood myeloid populations including Ly6G<sup>+</sup> neutrophils, CCR2<sup>+</sup>Ly6C<sup>hi</sup> and Ly6C<sup>Lo</sup> monocytes (Fig 4E).

In parallel to blood leukocyte analysis, colonic lamina propria leukocytes were isolated from the colon and characterized by flow cytometry (Fig 5A). Interestingly, despite the significant mobilization of myeloid cells to the bloodstream in response to CoPP, this did not translate into increased trafficking to the colon in active inflammation (Fig. 5B). Instead, we observed a significant numerical decrease in CD11b<sup>+</sup> myeloid cells in colitic mice treated with CoPP and a non-significant numerical decrease in CD45<sup>+</sup> leukocytes. Despite being greatly expanded in the blood, monocytes were markedly diminished in the colon of the colitic mice treated with CoPP (Fig. 5C). In colitic mice, we observed a reversal of macrophage expansion in CoPP treated mice compared to vehicle treated mice (Fig 5C), likely secondary to decreased monocyte precursors. We further examined the significance of disrupted monocyte trafficking towards the colon by comparing numbers of isolated colonic monocytes with measures of clinical inflammation, using our disease activity index (Fig 5D). We found a strong correlation between monocytes and disease activity, consistent with their reported importance in driving inflammation in this model (19, 20, 38). Infiltrating monocytes are also a major source of key inflammatory cytokines (e.g. IL-1 $\beta$  and TNF), with the former reported as a major contributor to inflammation in DSS and other colitis models (21, 22, 39–41). Importantly, in our CoPP treated mice, we observed a marked reduction of these key regulators of inflammation at the height of DSS injury correlating with diminished monocyte ( $r = .77, p = .0001$ ) and macrophage ( $r = .79, p < .0001$ ) populations (Fig. 5E).

These findings were similarly observed in the *Hmox1*<sup>fl/fl</sup>/LysMcre mice (Fig. S4) where we observed a parallel decrease in the numbers of colonic myeloid cells in the colitic mice treated with CoPP (Fig. S4A). These populations included monocytes, macrophages and to a lesser extent dendritic cells (Fig. S4B–C). Opposite shifts in myeloid populations were again seen in the circulating leukocytes (Fig. S4D), a development which has been shown to be independent of HO-1 (15).

### CoPP elicits a selective anti-inflammatory CCL2 gradient response

Based on the unexpected population shifts of monocytes between blood and colon, we hypothesized the likely disruption of chemotactic signaling by CoPP. CCR2 expression on Ly6C<sup>hi</sup> monocytes and binding of the ligand, CCL2, create a signaling axis that is critical to monocyte mobilization and recruitment from the bone marrow to the tissue (42). To address this signaling axis in relationship to CoPP, we collected colonic tissue and blood serum at the height of DSS injury and measured CCL2 concentration. In response to DSS injury, we observed significant increases in colonic expression of CCL2 (Fig. 6A). In CoPP treated mice we observed a similar increased level of CCL2 (Fig. 6A) in the healthy and the colitic mice. Prior work has noted an increase in serum CCL2 in healthy mice treated with CoPP (15). Our results replicated this finding (Fig. 6A).

Chemokine signaling is complex and involves sequestration of tissue chemokines by glycosaminoglycans to establish gradients, as well as binding and presentation by

endothelial cells to trigger leukocyte attachment and extravasation (43, 44). The magnitude of the concentration gradient dictates the efficiency of leukocyte migration towards the source. We utilized a simple measure of the magnitude of the concentration gradient between the colon lamina propria and blood by dividing our CCL2 (per mg total protein) levels in the colon by the same in the blood. We found that there was a significant increase in the CCL2 concentration gradient in vehicle treated colitic mice, but this increase was suppressed in colitic mice treated with CoPP (Fig. 6B). We found a strong correlation between the magnitude of this gradient and DAI score (Fig. 6C). We examined a limited panel of other pertinent chemokines regulating myeloid traffic to the colon such as CXCL1, CXCL2, and CCL11 and did not see a significant change in the chemoattractant gradient in response to CoPP treatment (Fig. S5), although decreased colonic CXCL1, and to a lesser extent CXCL2, likely contribute to the less significant decreased colonic neutrophil recruitment (Figure 5C).

Interestingly, we found that in CoPP treated mice, there was significantly decreased surface expression of CCR2 in blood Ly6C<sup>hi</sup> monocytes as measured by flow cytometry (Fig. 6D). This CCR2 expression also strongly correlated with disease activity in our colitis model (Fig. 6E). Given a recent report demonstrating a fine balance between CCR2 and CCL2 levels in the blood (45), we hypothesized that the decreased CCR2 expression was likely secondary to internalization of the receptor in the setting of sustained high levels of blood CCL2 (Fig. 6A). To examine this, we obtained fresh whole blood leukocytes from WT mice and exposed them to similar concentrations of CCL2 seen in serum taken from our vehicle and CoPP treated colitic mice (Fig. 6F). Gating on Ly6C<sup>hi</sup> monocytes we saw that within 30 minutes there was significantly reduced surface CCR2 in a CCL2 concentration dependent manner (Fig. 6G). A strong *in vivo* correlation between serum CCL2 and CCR2 expression on Ly6C<sup>hi</sup> monocytes analyzed in our colitis experiments further confirmed this relationship (Fig. 6H).

To determine a source for the increased circulating CCL2 we looked at CCL2 production in the spleen and liver where it has been previously described in the setting of erythrophagocytosis (46). While there was a modest increase in liver CCL2 in response to CoPP exposure, this was not markedly higher than the production from vehicle treated mice (Fig. 6I). However, we found markedly higher splenic levels of CCL2 in all CoPP treated mice compared to controls, and even more so in mice that received DSS (Fig. 6I). Systemic CoPP also elicited increased CCL2 in the lung, suggesting a more universal tissue response.

We attempted to neutralize circulating CCL2 in our CoPP treated mice using an IP delivered anti-CCL2 antibody, to determine if this could restore the natural gradient towards the colon. However, as previously described in human and murine studies, antibody neutralization of CCL2 is effective only transiently as it is followed by a robust and compensatory increase in CCL2 production that is not well understood (47–49). We observed the same increase in serum CCL2 levels (>4 fold increase at DSS day 5 comparing CoPP vs CoPP + anti-CCL2) in this setting and therefore saw no clinical difference from antibody neutralization.

## Discussion

Overall, our findings identify novel protective mechanisms for CoPP in intestinal inflammation. In the setting of colitis, the anti-inflammatory mechanism of CoPP was mostly understood to be through its influence on monocyte/macrophage HO-1. Our work examines this question head-on, and we reveal that myeloid HO-1 does not regulate the response to acute colitis. More complex heme-regulated pathways appear to be active in the context of CoPP treatment. CoPP appears to act as a mimic of heme, similar to results observed in the liver in the setting of hemolysis/erythrophagocytic stress, activating NRF2 associated differentiation of macrophages into anti-inflammatory erythrophagocytes (25). These liver macrophages can reportedly be identified by markers including high expression of *Hmox1*, *Marc0* and reduced expression of MHC class II, which we now report is also the case in the colon and in M-CSF cultured BMMs in response to CoPP. In this setting, HO-1 is not the critical effector protein but rather a functional marker of a distinctive population of anti-inflammatory macrophages. The anti-inflammatory influence of HO-1 in macrophages is supported by our findings in HO-1 deficient BMMs and ex vivo colonic macrophages in response to LPS, but in vivo, its importance is apparently less significant in the more complex colonic inflammatory environment and likely depends on the inflammatory model and tissue studied (36, 37). Other anti-inflammatory pathways may be concurrently active and predominate. Indeed, myeloid HO-1 dependent and independent factors are active in response to treatment with heme in similar settings (50, 51). Alternatively, it's also possible that sources of non-myeloid HO-1 may contribute to the anti-inflammatory influence of CoPP (52).

Regarding other anti-inflammatory pathways, our findings suggest that regulation of monocyte mobilization and trafficking plays a major role in the protective benefit of CoPP observed. Prior studies support a foremost role for monocytes in driving inflammation in DSS colitis (19, 20, 38). Reduced monocyte recruitment to the colon would therefore result in improved measures of disease/injury, which we observed. While the protective influence of CoPP may also derive from the distinct anti-inflammatory differentiation of colonic macrophages, we observed that the overall number of macrophages was diminished relative to vehicle treated colitic controls. Our analysis of the lamina propria monocyte and macrophage populations in the setting of CoPP treatment is consistent with the observation that circulating Ly6C<sup>hi</sup> monocytes replenish the intestinal macrophage pool (53, 54). In the setting of inflammation, these monocytes differentiate into inflammatory antigen presenting effector cells with macrophage and dendritic cell phenotypes (19, 24). Diminished monocyte recruitment therefore is expected to impact monocyte-derived downstream populations as well as contribute to diminished levels of cytokines they produce, which we observed. Our findings clearly support that CoPP diminishes colonic inflammatory monocyte and macrophage populations despite the robust recruitment of the former to the bloodstream.

Chemokines and chemokine receptors are key to the recruitment of myeloid populations to the colon in response to injury (55–58). The importance of this signaling is seen in CCL2-deficient and CCR2-deficient mice, where decreased colonic inflammation was observed in colitis models along with altered monocyte-macrophage populations (19, 38, 59). The sustained high levels of blood CCL2, in our CoPP treated mice, explain the significant

mobilization of monocytes from the bone marrow to the circulation, which is CCR2 dependent (42). Similar to other chemokine receptors CCR2 is a 7-transmembrane helical G-protein-coupled receptor that is rapidly internalized upon binding of its ligand, CCL2 (45, 60). It is rapidly cycled back to the plasma membrane to allow for optimal responsiveness to changes in the CCL2 gradient (60). Prior work has clearly shown decreased chemotactic responsiveness of mouse monocytes to CCL2 after significant internalization of CCR2, despite receptor recycling (61, 62). We found that high blood CCL2 levels mechanistically clarify the reduced recruitment of monocytes to the colon through a combination of diminished chemoattractant gradient strength towards the colon and decreased monocyte surface CCR2 expression. A weaker gradient and less receptors to perceive that gradient would be expected to impact the chemotactic response. Elevated concentrations of CCL2 also increase the number of recycled and less responsive CCR2 receptors (61, 62). This highlights the disruption by CoPP of a very important and interesting balancing act for blood CCL2 levels with regards to recruitment and subsequent tissue delivery of monocytes (45).

Phagocytosis of aged or damaged red blood cells by RPMs in the spleen elicits the production of CCL2 and CCL7 by splenic Ly6C<sup>hi</sup> monocytes as the red blood cells are metabolized. This results in the recruitment of bone marrow monocytes to assist in replenishing dead or dying RPMs (46, 63). A proposed signal for this production of CCL2 is free heme elaborated from red cell degradation and breakdown of hemoglobin (63). Given the similar signaling between heme and CoPP, we examined splenic production of CCL2 in the setting of CoPP treatment and inflammation. We found markedly increased production of splenic CCL2 after CoPP exposure and a similar response was seen in organs such as lung and to a lesser extent, liver. These results further implicate CoPP as a mimic of heme observed in the setting of hemolysis/erythrophagocytic stress, in this case leading to a potent CCL2 response resulting in an anti-inflammatory impact in the setting of inflammation.

One limitation of this work is that we focused on acute inflammation while the contribution of protective mechanisms of myeloid HO-1 and CoPP may differ in models of chronic mucosal inflammation where leukocyte recruitment patterns differ. However, DSS colitis is a good model for evaluating the contribution of the innate immune system to intestinal inflammation. Additionally, there are potentially different mechanisms underlying the potent protective influence of the HO-1 metabolic product carbon monoxide vs CoPP, which we did not assess. For example, in strong contrast to our findings, it has been shown that CO suppresses tissue CCL2 production and inhibits monocyte CCR2 internalization in a murine model of acute pancreatitis (64). Given the efficacy of CoPP and heme in a wide range of acute and chronic inflammatory murine models of disease, identifying specific and consistent mechanisms may facilitate better translation of experimental findings to therapeutic applications in humans.

## Materials and methods

### DSS colitis.

C57BL/6 *Hmox1*<sup>fl/fl</sup> mice were kindly provided by Dr. H. B. Suliman (65). HO-1 Myeloid mice, which have been previously described (36), were made by crossing *Hmox1*<sup>fl/fl</sup> mice with *Lyz2-cre/LysMcre* mice (JAX) (66). Both *Hmox1*<sup>fl/fl</sup> and *LysMcre* mice served

as controls given they were phenotypically identical in preliminary experiments. Lavage recovery of peritoneal cells showed an 86.5% average reduction in *Hmox1* expression comparing controls (n=3) to HO-1<sup>Myeloid</sup> mice (n=3;  $p = .0005$ ). All mice were maintained and handled in accordance with Institutional Animal Care and Use Guidelines. Littermate controls were used for all colitis experiments in WT and transgenic mice with regard to treatment groups. *Hmox1*<sup>fl/fl</sup> mice were caged separately from *Hmox1*<sup>fl/fl</sup>/LysMcre mice. Age-matched male and female mice were used between age 7 and 14 weeks. Mice were given 2.5% colitis grade dextran sodium sulfate (DSS, MP Biomedical) in drinking water, changed every 2 days, for 5 days. DSS was removed on day 5 from all colitis experiments and mice were sacrificed on day 5 or day 7, where noted. Mice were injected with 7.5mg/kg cobalt(III) protoporphyrin IX chloride (CoPP, Frontier Scientific) where noted, on days 0, 2, and 4 of treatment. Mice were weighed daily, and fecal pellets scored for stool consistency and presence of blood; all measured on a scale of 0–3 and blinded as to treatment. Disease Activity Index (DAI) was then calculated by taking the summation of weight change, stool consistency and hematochezia scores (maximum score of 9). At experiment end, colons were embedded and processed for histology. H&E stained tissue was scored by a histopathologist blinded to the treatments and groupings of animals using described methods (67). To block CCL2 we used an *In Vivo*MAB anti-CCL2 antibody (2H5 clone; BioXCell) at 75 µg every 48 starting day 0 in a 5 days DSS experiment with *In Vivo*MAB polyclonal Armenian hamster IgG control.

### Leukocyte isolation.

Isolation of colonic lamina propria cells was adapted from a previously described protocol (68). After dissociation of the epithelial layer for 10 minutes x3 at room temp, remaining colon tissue was minced using scissors and digested in media with 500ug/mL of DNASE I (Sigma Aldrich) and 1mg/mL of Collagenase type IV (Worthington Biochemical Company). Digested tissue was filtered sequentially through 100 µm and 40 µm filters followed by centrifugation and resuspension in buffer for subsequent staining. Blood leukocytes were isolated after retro-orbital collection of whole blood, followed by RBC lysis and staining for flow cytometry. In one experiment, fresh blood leukocytes were exposed to recombinant mouse CCL2 (Biolegend) in RPMI complete media (RPMI-1640, 10%FBS, 1%Pen/Strep) and incubated in 95% air with 5% CO<sub>2</sub> at 37°C for 1 hour.

### Chemokine assays.

Whole colon tissue isolated from the distal colon was homogenized in MSD lysis buffer (150mM NaCl, 20mM Tris pH 7.5, 1mM EDTA, 1mM EGTA, 1% Triton X-100) with 1x phosphatase and protease inhibitors (Thermo Fischer Scientific). Portions of whole spleen, liver and lung were also isolated and processed in the same manner for chemokine assays. Serum for chemokine assays was isolated from whole blood collected through retro-orbital bleed. All tissue chemokine concentrations were normalized against total protein using Pierce™ BCA Protein Assay kit (Thermo-Fisher Scientific). Initial ELISA was performed using custom mouse U-Plex Assays (Meso Scale Discovery). Additional ELISA assays performed included CCL2/JE/MCP1 (DuoSet ELISA assay, R&D Systems), and Mouse CCL11 Legend Max™ Elisa (Biolegend) all normalized to total protein. In a select experiment distal colon tissue was collected and homogenized in MSD lysis buffer/

protease inhibitor for a 92-plex proteomic analysis of which 75 targets were detected (Olink Proteomics) (69).

### Flow cytometry.

Flow cytometry was used to characterize leukocyte populations in the blood and colon based on total cell counts. Cell isolations for flow cytometry were stained with antibodies purchased from Biolegend. All cells were stained with Biolegend 7AAD Viability Staining Solution prior to flow analysis. Biolegend TruStain FcX (anti-mouse CD16/32) antibody was used for blocking. The following anti-mouse antibodies were used for colonic leukocyte or blood myeloid leukocyte staining: anti-CD64 (clone X54-4/7.1), anti-CD170/Siglec-F (S17007L), anti-MHC-II (M5/114.15.2), anti-CD11c (N418), anti-CD45 (30-F11), anti-Ly6C (HK1.4), anti-CD11b (M1/70), anti-Ly6G (1A8), anti-CD192/CCR2 (SA203G11), anti-CX3CR1 (SA011F11). Bone marrow-derived macrophage cultures were stained with the following antibodies from Biolegend: anti-F4/80 (BM8), anti-CD11b (M1/70), and mouse anti-Marco (579511) from Bio-Techne/R&D Systems. Flow cytometry was performed on a FACSCanto™ II (Becton Dickinson), or a BD FACSAria™ Fusion and resulting data was analyzed with De Novo's FCS Express 7 software.

### In vitro/ex vivo macrophage experiments.

Bone marrow-derived macrophages (BMMs) were isolated as follows: Mouse femoral and tibial bone marrow was flushed out using a 25g needle and syringe with RPMI-1640 media onto a 70µm filter. Cells were centrifuged and washed with RPMI-1640 after RBC lysis. Cells were cultured in RPMI complete media (RPMI-1640, 10%FBS, 1%Pen/Strep) and incubated in 95% air with 5% CO<sub>2</sub> at 37°C. Recombinant murine M-CSF (PeproTech US) was at 20 to 40ng/mL to differentiate to macrophages from day 0 to day 6. M1 macrophages were further differentiated by exposure of BMMs to 24 hours of 1ng/mL LPS (Millipore Sigma) and 10ng/mL of recombinant mouse IFN $\gamma$  (Biolegend). After M1 differentiation, 25µM CoPP and 10ng/mL of LPS was added to the BMMs for another 24 hours. For some BMM experiments, cells were treated with 25µM CoPP for 24 hours and then stimulated with 50ng/mL LPS for 2 hours. For flow cytometry, BMMs were treated with 25µM CoPP or 10ng LPS for 24 hours. For ex vivo colonic macrophages, 2h culture was performed with LPS 25ng/mL in the same media used for BMMs but without M-CSF or cytokine stimulation.

### Reverse transcription-quantitative PCR (qPCR).

RNA was isolated from snap frozen tissue samples and BMMs using the Qiagen RNeasy Mini kit with the addition of the gDNA-eliminator columns as per manufacturer's protocol. First-strand complementary DNA synthesis was performed with 1 µg of total RNA using iScript reverse transcription super-mix from Bio-Rad. Real-time qPCR was performed using SYBR green on an ABI 7900HT fast real-time PCR system (both from Applied Biosystems).  $\beta$ -Actin (ACTB) was used as the housekeeping gene. The primer sequence for beta-actin purchased from Invitrogen was: ACTB, sense 5'-CACTCTTCCAGCCTTCCTTCC-3', antisense 5'-CAGGTCTTTGCGGATGTCCACG-3'. All other mouse primer sets were purchased from Sigma-Aldrich's line of KiCqStart™ Primers: *Ccl2*, *Hmox1*, *Il1b*, *Il6*, *Marco*, *Nos2 (iNos)*, *Slc40a1*, *Spic*, *Tnf*, *Il12b* and *Cxcl10*.

## RNA-Seq.

RNA was isolated using TRIzol reagent (Invitrogen) and Qiagen RNeasy kit was also utilized subsequently to improve purity. Eukaryotic RNA-sequencing was carried out on the Illumina NovaSeq 6000 system (Novogene Corporation Inc.). Reference genome and gene model annotation files were downloaded from genome website browser (NCBI/UCSC/Ensembl) directly. Indexes of the reference genome was built using STAR and paired-end clean reads were aligned to the reference genome using STAR (v2.5). HTSeq v0.6.1 was used to count the read numbers mapped of each gene. And then FPKM of each gene was calculated based on the length of the gene and reads count mapped to this gene. Alignments were parsed using Tophat program and differential expressions were determined through DESeq2/EdgeR. GO and KEGG enrichment were implemented by the ClusterProfiler. Additional analysis was performed using iDEP, a web-based tool for analyzing RNA-seq data (70). Parameters for DEG analyses (DESeq2) included FDR cutoff of 0.1 and minimum fold change of 2.

## Immunohistochemistry.

Paraffin embedded tissues were deparaffinized using two 100% xylene washes for 5 minutes followed by sequential 3 minute washes in 1:1 xylene:Ethanol, 100%, 95%, 70%, and 50% ethanol. Tissues were then rinsed and placed in a staining box with Tris-EDTA buffer pH 9.0 (10mM Tris Base, 1mM EDTA solution, 0.05% TWEEN®20). Heat induced epitope retrieval was performed at 95°C in a pressure cooker for 25 minutes. After rinsing in 1x TBST buffer (Tris-buffered saline, 0.2% TWEEN®20) slides were blocked with 10% normal goat serum (Thomas Scientific) in PBS for 1 hour. After 1x TBST rinse, staining was performed with rabbit polyclonal HO-1 antibody (Enzo Life Sciences), and rat monoclonal [CI:A3-1] F4/80 antibody (Abcam) 4°C overnight in a humidified chamber. After rinsing, secondary antibodies goat anti-rabbit AF-555 and goat anti-rat AF-488 (Invitrogen), were applied for 2 hours at room temperature in a humidified chamber. Slides were rinsed then sealed with Molecular Probes™ ProLong™ Diamond Antifade Mountant with or without DAPI (Fischer Scientific). Imaging was done on an Olympus IX83P2F microscope equipped with a DP80 camera. Additional images were obtained on an AxioImager A1 microscope (Zeiss) equipped with an AxioCam MRc5.

## Statistical analyses:

Where appropriate, unpaired, two-tailed Student's *t* test or one-way ANOVA (for more than two groups) with correction for multiple comparisons (two-stage linear step-up procedure of Benjamini, Krieger and Yekutieli) was performed using Prism version 9 (GraphPad Software). DAI scores were analyzed using a mixed-effects model. Results were considered statistically significant when  $p < .05$ .

## Supplementary Material

Refer to Web version on PubMed Central for supplementary material.

## Acknowledgements

The authors would like to thank T. Nguyen and M. Minhajuddin (Department of Medicine, University of Colorado) for helpful comments regarding flow cytometry. We thank Sarah Williams for help with animal husbandry. This work was supported by a VA Career Development Award (BX003865), Univ. of Colorado GI and Liver Innate Immune Program pilot award to J.C.O.; VA Merit (BX002182) and NIH awards to S.P.C.

## References

1. Alam J, Stewart D, Touchard C, Boinapally S, Choi AM, Cook JL. Nrf2, a Cap'n'Collar transcription factor, regulates induction of the heme oxygenase-1 gene. *J Biol Chem.* 1999;274(37):26071–8. [PubMed: 10473555]
2. Bonkovsky HL, Guo JT, Hou W, Li T, Narang T, Thapar M. Porphyrin and heme metabolism and the porphyrias. *Compr Physiol.* 2013;3(1):365–401. [PubMed: 23720291]
3. Wong RJ, Vreman HJ, Schulz S, Kalish FS, Pierce NW, Stevenson DK. In vitro inhibition of heme oxygenase isoenzymes by metalloporphyrins. *J Perinatol.* 2011;31 Suppl 1:S35–41. [PubMed: 21448202]
4. Shan Y, Pepe J, Lu TH, Elbirt KK, Lambrecht RW, Bonkovsky HL. Induction of the heme oxygenase-1 gene by metalloporphyrins. *Arch Biochem Biophys.* 2000;380(2):219–27. [PubMed: 10933875]
5. Hoffman BM, Petering DH. Coboglobins: oxygen-carrying cobalt-reconstituted hemoglobin and myoglobin. *Proc Natl Acad Sci U S A.* 1970;67(2):637–43. [PubMed: 4331717]
6. Vernon DI, Brown SB. Formation of bile pigments by coupled oxidation of cobalt-substituted haemoglobin and myoglobin. *Biochem J.* 1984;223(1):205–9. [PubMed: 6497839]
7. Yonetani T, Yamamoto H, Woodrow GV 3rd. Studies on cobalt myoglobins and hemoglobins. I. Preparation and optical properties of myoglobins and hemoglobins containing cobalt proto-, meso-, and deuteroporphyrins and thermodynamic characterization of their reversible oxygenation. *J Biol Chem.* 1974;249(3):682–90. [PubMed: 4855813]
8. Shan Y, Lambrecht RW, Donohue SE, Bonkovsky HL. Role of Bach1 and Nrf2 in up-regulation of the heme oxygenase-1 gene by cobalt protoporphyrin. *FASEB J.* 2006;20(14):2651–3. [PubMed: 17065227]
9. Ryter SW. Therapeutic Potential of Heme Oxygenase-1 and Carbon Monoxide in Acute Organ Injury, Critical Illness, and Inflammatory Disorders. *Antioxidants (Basel).* 2020;9(11).
10. Paul G, Bataille F, Obermeier F, Bock J, Klebl F, Strauch U, et al. Analysis of intestinal haem-oxygenase-1 (HO-1) in clinical and experimental colitis. *Clin Exp Immunol.* 2005;140(3):547–55. [PubMed: 15932518]
11. Onyiah JC, Sheikh SZ, Maharshak N, Steinbach EC, Russo SM, Kobayashi T, et al. Carbon monoxide and heme oxygenase-1 prevent intestinal inflammation in mice by promoting bacterial clearance. *Gastroenterology.* 2013;144(4):789–98. [PubMed: 23266559]
12. Sheikh SZ, Hegazi RA, Kobayashi T, Onyiah JC, Russo SM, Matsuoka K, et al. An anti-inflammatory role for carbon monoxide and heme oxygenase-1 in chronic Th2-mediated murine colitis. *J Immunol.* 2011;186(9):5506–13. [PubMed: 21444764]
13. Hegazi RA, Rao KN, Mayle A, Sepulveda AR, Otterbein LE, Plevy SE. Carbon monoxide ameliorates chronic murine colitis through a heme oxygenase 1-dependent pathway. *J Exp Med.* 2005;202(12):1703–13. [PubMed: 16365149]
14. Marelli G, Erreni M, Anselmo A, Taverniti V, Guglielmetti S, Mantovani A, et al. Heme-oxygenase-1 Production by Intestinal CX3CR1(+) Macrophages Helps to Resolve Inflammation and Prevents Carcinogenesis. *Cancer Res.* 2017;77(16):4472–85. [PubMed: 28619710]
15. Szade A, Szade K, Nowak WN, Bukowska-Strakova K, Muchova L, Gonka M, et al. Cobalt protoporphyrin IX increases endogenous G-CSF and mobilizes HSC and granulocytes to the blood. *EMBO Mol Med.* 2019;11(12):e09571. [PubMed: 31709729]
16. Okayasu I, Hatakeyama S, Yamada M, Ohkusa T, Inagaki Y, Nakaya R. A novel method in the induction of reliable experimental acute and chronic ulcerative colitis in mice. *Gastroenterology.* 1990;98(3):694–702. [PubMed: 1688816]

17. Chassaing B, Aitken JD, Malleshappa M, Vijay-Kumar M. Dextran sulfate sodium (DSS)-induced colitis in mice. *Curr Protoc Immunol.* 2014;104:15 25 1–15 25 14. [PubMed: 24510619]
18. Luissint AC, Parkos CA, Nusrat A. Inflammation and the Intestinal Barrier: Leukocyte-Epithelial Cell Interactions, Cell Junction Remodeling, and Mucosal Repair. *Gastroenterology.* 2016;151(4):616–32. [PubMed: 27436072]
19. Zigmond E, Varol C, Farache J, Elmaliah E, Satpathy AT, Friedlander G, et al. Ly6C hi monocytes in the inflamed colon give rise to proinflammatory effector cells and migratory antigen-presenting cells. *Immunity.* 2012;37(6):1076–90. [PubMed: 23219392]
20. Platt AM, Bain CC, Bordon Y, Sester DP, Mowat AM. An independent subset of TLR expressing CCR2-dependent macrophages promotes colonic inflammation. *J Immunol.* 2010;184(12):6843–54. [PubMed: 20483766]
21. Jones GR, Bain CC, Fenton TM, Kelly A, Brown SL, Ivens AC, et al. Dynamics of Colon Monocyte and Macrophage Activation During Colitis. *Front Immunol.* 2018;9:2764. [PubMed: 30542349]
22. Seo SU, Kamada N, Munoz-Planillo R, Kim YG, Kim D, Koizumi Y, et al. Distinct Commensals Induce Interleukin-1beta via NLRP3 Inflammasome in Inflammatory Monocytes to Promote Intestinal Inflammation in Response to Injury. *Immunity.* 2015;42(4):744–55. [PubMed: 25862092]
23. Flannigan KL, Geem D, Harusato A, Denning TL. Intestinal Antigen-Presenting Cells: Key Regulators of Immune Homeostasis and Inflammation. *Am J Pathol.* 2015;185(7):1809–19. [PubMed: 25976247]
24. Rivollier A, He J, Kole A, Valatas V, Kelsall BL. Inflammation switches the differentiation program of Ly6Chi monocytes from antiinflammatory macrophages to inflammatory dendritic cells in the colon. *J Exp Med.* 2012;209(1):139–55. [PubMed: 22231304]
25. Pfefferle M, Ingoglia G, Schaer CA, Yalamanoglu A, Buzzi R, Dubach IL, et al. Hemolysis transforms liver macrophages into antiinflammatory erythrophagocytes. *J Clin Invest.* 2020;130(10):5576–90. [PubMed: 32663195]
26. Elomaa O, Kangas M, Sahlberg C, Tuukkanen J, Sormunen R, Liakka A, et al. Cloning of a novel bacteria-binding receptor structurally related to scavenger receptors and expressed in a subset of macrophages. *Cell.* 1995;80(4):603–9. [PubMed: 7867067]
27. Ito S, Naito M, Kobayashi Y, Takatsuka H, Jiang S, Usuda H, et al. Roles of a macrophage receptor with collagenous structure (MARCO) in host defense and heterogeneity of splenic marginal zone macrophages. *Arch Histol Cytol.* 1999;62(1):83–95. [PubMed: 10223745]
28. van der Laan LJ, Dopp EA, Haworth R, Pikkarainen T, Kangas M, Elomaa O, et al. Regulation and functional involvement of macrophage scavenger receptor MARCO in clearance of bacteria in vivo. *J Immunol.* 1999;162(2):939–47. [PubMed: 9916718]
29. Palecanda A, Paulauskis J, Al-Mutairi E, Imrich A, Qin G, Suzuki H, et al. Role of the scavenger receptor MARCO in alveolar macrophage binding of unopsonized environmental particles. *J Exp Med.* 1999;189(9):1497–506. [PubMed: 10224290]
30. Bain CC, Schridde A. Origin, Differentiation, and Function of Intestinal Macrophages. *Frontiers in Immunology.* 2018;9. [PubMed: 29403493]
31. Medina-Contreras O, Geem D, Laur O, Williams IR, Lira SA, Nusrat A, et al. CX3CR1 regulates intestinal macrophage homeostasis, bacterial translocation, and colitogenic Th17 responses in mice. *J Clin Invest.* 2011;121(12):4787–95. [PubMed: 22045567]
32. Haldar M, Kohyama M, So AY, Kc W, Wu X, Briseno CG, et al. Heme-mediated SPI-C induction promotes monocyte differentiation into iron-recycling macrophages. *Cell.* 2014;156(6):1223–34. [PubMed: 24630724]
33. Ueda Y, Kayama H, Jeon SG, Kusu T, Isaka Y, Rakugi H, et al. Commensal microbiota induce LPS hyporesponsiveness in colonic macrophages via the production of IL-10. *Int Immunol.* 2010;22(12):953–62. [PubMed: 21051439]
34. Soares MP, Hamza I. Macrophages and Iron Metabolism. *Immunity.* 2016;44(3):492–504. [PubMed: 26982356]

35. Kovtunovych G, Eckhaus MA, Ghosh MC, Ollivierre-Wilson H, Rouault TA. Dysfunction of the heme recycling system in heme oxygenase 1-deficient mice: effects on macrophage viability and tissue iron distribution. *Blood*. 2010;116(26):6054–62. [PubMed: 20844238]
36. Tzima S, Victoratos P, Kranidioti K, Alexiou M, Kollias G. Myeloid heme oxygenase-1 regulates innate immunity and autoimmunity by modulating IFN-beta production. *J Exp Med*. 2009;206(5):1167–79. [PubMed: 19398754]
37. Zhang M, Nakamura K, Kageyama S, Lawal AO, Gong KW, Bhetraratana M, et al. Myeloid HO-1 modulates macrophage polarization and protects against ischemia-reperfusion injury. *JCI Insight*. 2018;3(19).
38. Waddell A, Ahrens R, Steinbrecher K, Donovan B, Rothenberg ME, Munitz A, et al. Colonic eosinophilic inflammation in experimental colitis is mediated by Ly6C(high) CCR2(+) inflammatory monocyte/macrophage-derived CCL11. *J Immunol*. 2011;186(10):5993–6003. [PubMed: 21498668]
39. Kwon KH, Murakami A, Hayashi R, Ohigashi H. Interleukin-1beta targets interleukin-6 in progressing dextran sulfate sodium-induced experimental colitis. *Biochem Biophys Res Commun*. 2005;337(2):647–54. [PubMed: 16202978]
40. Arai Y, Takanashi H, Kitagawa H, Okayasu I. Involvement of interleukin-1 in the development of ulcerative colitis induced by dextran sulfate sodium in mice. *Cytokine*. 1998;10(11):890–6. [PubMed: 9878126]
41. Neudecker V, Haneklaus M, Jensen O, Khailova L, Masterson JC, Tye H, et al. Myeloid-derived miR-223 regulates intestinal inflammation via repression of the NLRP3 inflammasome. *J Exp Med*. 2017;214(6):1737–52. [PubMed: 28487310]
42. Serbina NV, Pamer EG. Monocyte emigration from bone marrow during bacterial infection requires signals mediated by chemokine receptor CCR2. *Nat Immunol*. 2006;7(3):311–7. [PubMed: 16462739]
43. Proudfoot AE, Handel TM, Johnson Z, Lau EK, LiWang P, Clark-Lewis I, et al. Glycosaminoglycan binding and oligomerization are essential for the in vivo activity of certain chemokines. *Proc Natl Acad Sci U S A*. 2003;100(4):1885–90. [PubMed: 12571364]
44. Crijns H, Vanheule V, Proost P. Targeting Chemokine-Glycosaminoglycan Interactions to Inhibit Inflammation. *Front Immunol*. 2020;11:483. [PubMed: 32296423]
45. Zhao BN, Campbell JJ, Salanga CL, Ertl LS, Wang Y, Yau S, et al. CCR2-Mediated Uptake of Constitutively Produced CCL2: A Mechanism for Regulating Chemokine Levels in the Blood. *J Immunol*. 2019;203(12):3157–65. [PubMed: 31676674]
46. Wojczyk BS, Kim N, Bandyopadhyay S, Francis RO, Zimring JC, Hod EA, et al. Macrophages clear refrigerator storage-damaged red blood cells and subsequently secrete cytokines in vivo, but not in vitro, in a murine model. *Transfusion*. 2014;54(12):3186–97. [PubMed: 25041478]
47. Haringman JJ, Gerlag DM, Smeets TJ, Baeten D, van den Bosch F, Bresnihan B, et al. A randomized controlled trial with an anti-CCL2 (anti-monocyte chemotactic protein 1) monoclonal antibody in patients with rheumatoid arthritis. *Arthritis Rheum*. 2006;54(8):2387–92. [PubMed: 16869001]
48. Raghu G, Martinez FJ, Brown KK, Costabel U, Cottin V, Wells AU, et al. CC-chemokine ligand 2 inhibition in idiopathic pulmonary fibrosis: a phase 2 trial of carlumab. *Eur Respir J*. 2015;46(6):1740–50. [PubMed: 26493793]
49. Zhao L, Lim SY, Gordon-Weeks AN, Tapmeier TT, Im JH, Cao Y, et al. Recruitment of a myeloid cell subset (CD11b/Gr1 mid) via CCL2/CCR2 promotes the development of colorectal cancer liver metastasis. *Hepatology*. 2013;57(2):829–39. [PubMed: 23081697]
50. Wu Y, Wu B, Zhang Z, Lu H, Fan C, Qi Q, et al. Heme protects intestinal mucosal barrier in DSS-induced colitis through regulating macrophage polarization in both HO-1-dependent and HO-1-independent way. *FASEB J*. 2020;34(6):8028–43. [PubMed: 32301543]
51. Konrad FM, Knausberg U, Hone R, Ngamsri KC, Reutershan J. Tissue heme oxygenase-1 exerts anti-inflammatory effects on LPS-induced pulmonary inflammation. *Mucosal Immunol*. 2016;9(1):98–111. [PubMed: 25943274]

52. Onyiah JC, Schaefer REM, Colgan SP. A Central Role for Heme Oxygenase-1 in the Control of Intestinal Epithelial Chemokine Expression. *J Innate Immun.* 2018;10(3):228–38. [PubMed: 29791903]
53. Bain CC, Bravo-Blas A, Scott CL, Perdiguero EG, Geissmann F, Henri S, et al. Constant replenishment from circulating monocytes maintains the macrophage pool in the intestine of adult mice. *Nat Immunol.* 2014;15(10):929–37. [PubMed: 25151491]
54. Bain CC, Scott CL, Uronen-Hansson H, Gudjonsson S, Jansson O, Grip O, et al. Resident and pro-inflammatory macrophages in the colon represent alternative context-dependent fates of the same Ly6Chi monocyte precursors. *Mucosal Immunol.* 2013;6(3):498–510. [PubMed: 22990622]
55. Zimmerman NP, Vongsa RA, Wendt MK, Dwinell MB. Chemokines and chemokine receptors in mucosal homeostasis at the intestinal epithelial barrier in inflammatory bowel disease. *Inflamm Bowel Dis.* 2008;14(7):1000–11. [PubMed: 18452220]
56. Kulkarni N, Pathak M, Lal G. Role of chemokine receptors and intestinal epithelial cells in the mucosal inflammation and tolerance. *J Leukoc Biol.* 2017;101(2):377–94. [PubMed: 27899415]
57. Gunaltay S, Kumawat AK, Nyhlin N, Bohr J, Tysk C, Hultgren O, et al. Enhanced levels of chemokines and their receptors in the colon of microscopic colitis patients indicate mixed immune cell recruitment. *Mediators Inflamm.* 2015;2015:132458. [PubMed: 25948880]
58. Singh UP, Singh NP, Murphy EA, Price RL, Fayad R, Nagarkatti M, et al. Chemokine and cytokine levels in inflammatory bowel disease patients. *Cytokine.* 2016;77:44–9. [PubMed: 26520877]
59. Khan WI, Motomura Y, Wang H, El-Sharkawy RT, Verdu EF, Verma-Gandhu M, et al. Critical role of MCP-1 in the pathogenesis of experimental colitis in the context of immune and enterochromaffin cells. *Am J Physiol Gastrointest Liver Physiol.* 2006;291(5):G803–11. [PubMed: 16728728]
60. Volpe S, Cameroni E, Moepps B, Thelen S, Apuzzo T, Thelen M. CCR2 acts as scavenger for CCL2 during monocyte chemotaxis. *PLoS One.* 2012;7(5):e37208. [PubMed: 22615942]
61. Handel TM, Johnson Z, Rodrigues DH, Dos Santos AC, Cirillo R, Muzio V, et al. An engineered monomer of CCL2 has anti-inflammatory properties emphasizing the importance of oligomerization for chemokine activity in vivo. *J Leukoc Biol.* 2008;84(4):1101–8. [PubMed: 18662971]
62. Carvallo L, Lopez L, Che FY, Lim J, Eugenin EA, Williams DW, et al. Buprenorphine decreases the CCL2-mediated chemotactic response of monocytes. *J Immunol.* 2015;194(7):3246–58. [PubMed: 25716997]
63. Youssef LA, Rebbaa A, Pampou S, Weisberg SP, Stockwell BR, Hod EA, et al. Increased erythrophagocytosis induces ferroptosis in red pulp macrophages in a mouse model of transfusion. *Blood.* 2018;131(23):2581–93. [PubMed: 29666112]
64. Wu J, Zhang R, Hu G, Zhu HH, Gao WQ, Xue J. Carbon Monoxide Impairs CD11b(+)Ly-6C(hi) Monocyte Migration from the Blood to Inflamed Pancreas via Inhibition of the CCL2/CCR2 Axis. *J Immunol.* 2018;200(6):2104–14. [PubMed: 29440506]
65. Suliman HB, Keenan JE, Piantadosi CA. Mitochondrial quality-control dysregulation in conditional HO-1(–/–) mice. *JCI Insight.* 2017;2(3):e89676. [PubMed: 28194437]
66. Clausen BE, Burkhardt C, Reith W, Renkawitz R, Forster I. Conditional gene targeting in macrophages and granulocytes using LysMcre mice. *Transgenic Res.* 1999;8(4):265–77. [PubMed: 10621974]
67. Dieleman LA, Palmén MJ, Akol H, Bloemena E, Pena AS, Meuwissen SG, et al. Chronic experimental colitis induced by dextran sulphate sodium (DSS) is characterized by Th1 and Th2 cytokines. *Clin Exp Immunol.* 1998;114(3):385–91. [PubMed: 9844047]
68. Couter CJ, Surana NK. Isolation and Flow Cytometric Characterization of Murine Small Intestinal Lymphocytes. *J Vis Exp.* 2016(111).
69. Assarsson E, Lundberg M, Holmquist G, Björkstén J, Thorsen SB, Ekman D, et al. Homogenous 96-plex PEA immunoassay exhibiting high sensitivity, specificity, and excellent scalability. *PLoS One.* 2014;9(4):e95192. [PubMed: 24755770]
70. Ge SX, Son EW, Yao R. iDEP: an integrated web application for differential expression and pathway analysis of RNA-Seq data. *BMC Bioinformatics.* 2018;19(1):534. [PubMed: 30567491]

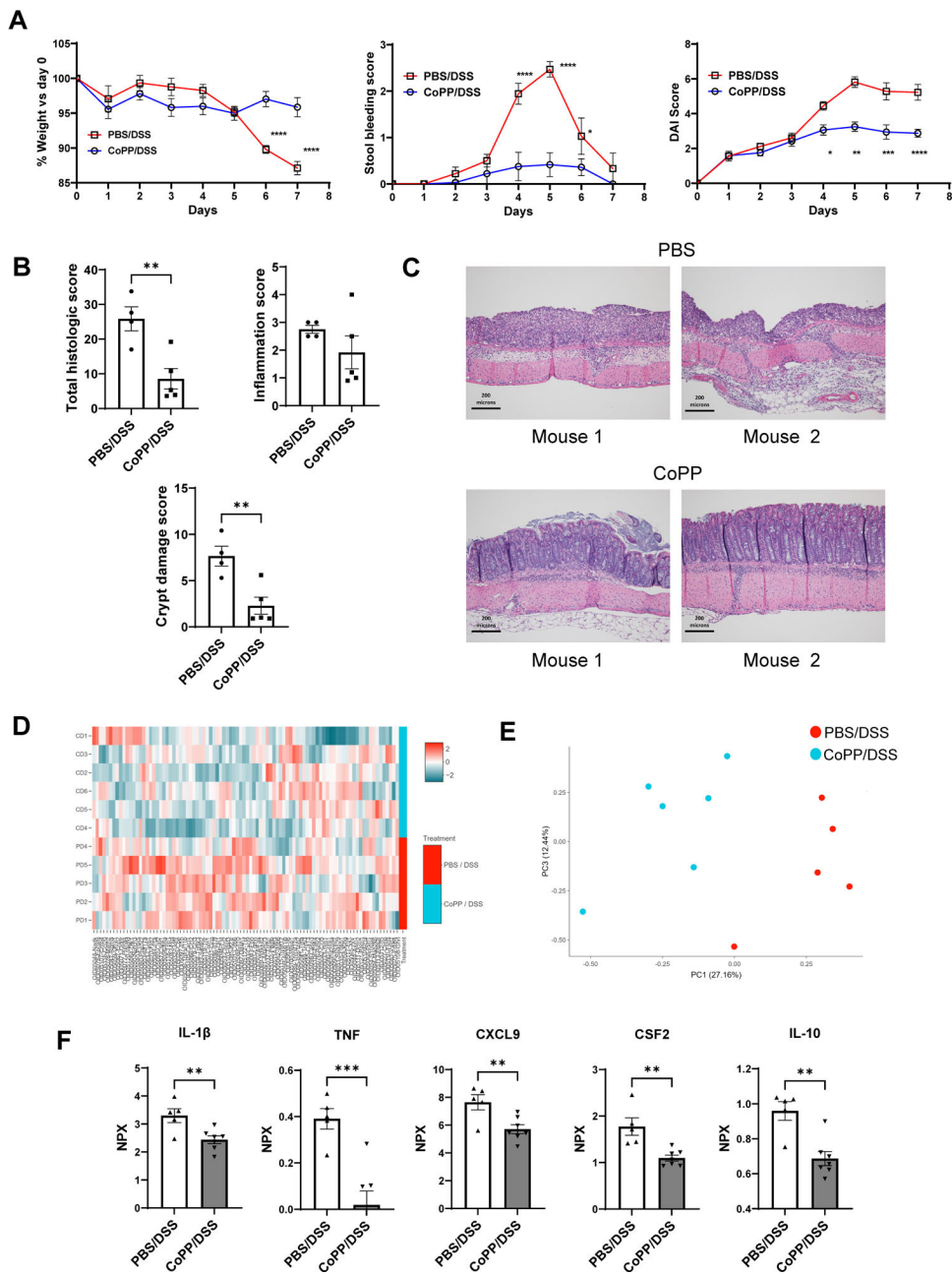


**Figure 1. Cobalt protoporphyrin protects against DSS induced intestinal inflammation.** (A) Percent weight loss, stool bleeding scores and combined disease activity index (DAI), from WT mice that received 2.5% DSS in their drinking water for 5 days. Mice were treated with vehicle or CoPP IP (n = 4 – 5 per group) on days 0, 2 and 4. (B) Histopathological score and select components from colon tissue harvested at day 7. (C) Representative microscopic images of hematoxylin and eosin stained colon tissue at day 7 of the DSS experiment. Results are representative of two or more independent experiments. (D) WT mice received 2.5% DSS for 5 days and were treated with PBS or CoPP IP. Whole colon tissue was recovered for proteomic analysis (n = 5 – 6). Heat map representation of protein expression encompassing 75 detectable targets. (E) Principal component analysis

with samples plotted based on the first and third principal components. (F) Normalized protein expression (NPX) of select individual genes with significant differences. \* $p < .05$ , \*\* $p < .01$ , \*\*\* $p < .001$ , \*\*\*\* $p < .0001$

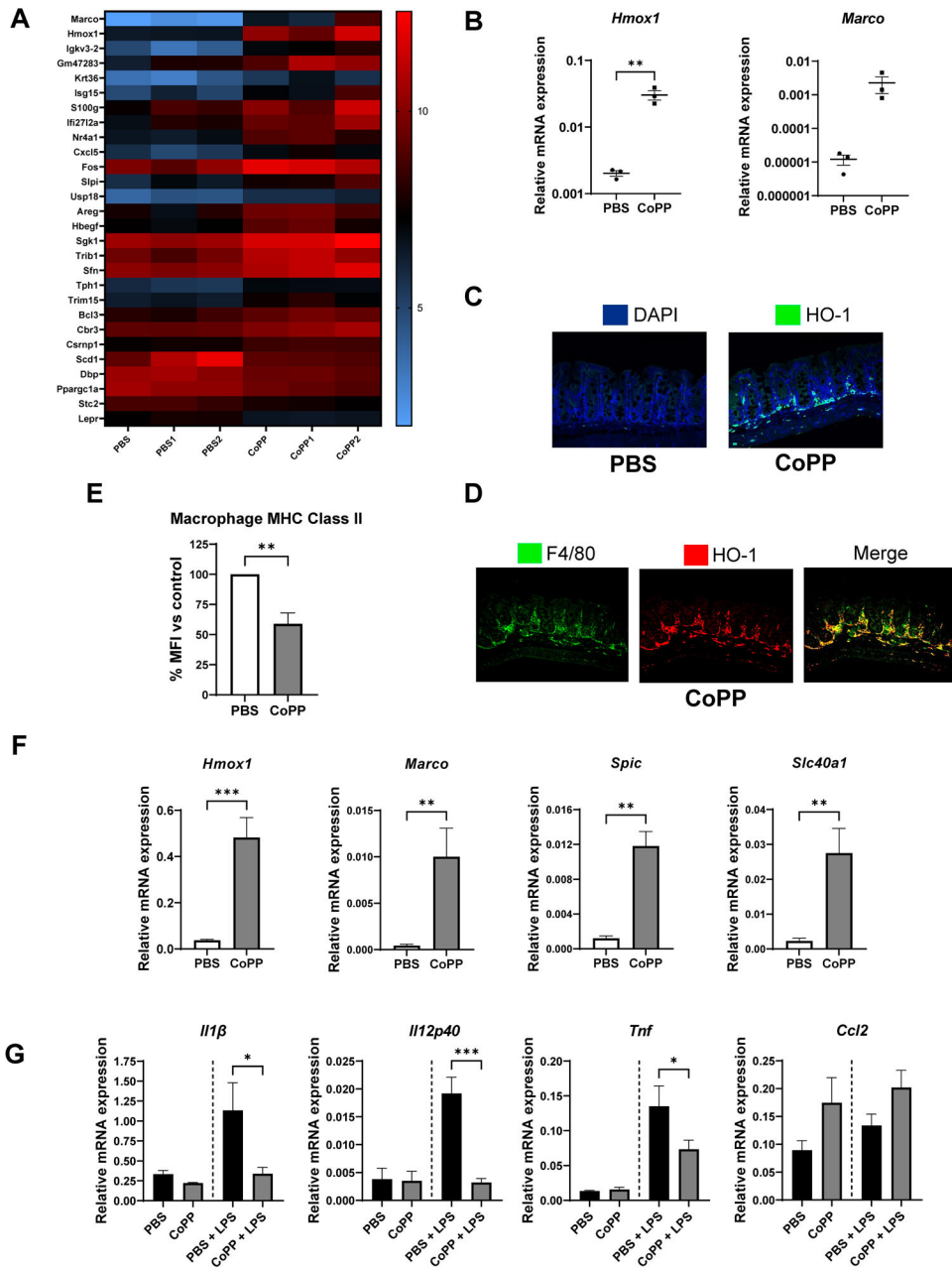


**Figure 2. Colonic transcriptome profile in response to CoPP exposure.** WT mice received drinking water for 5 days along with either PBS or CoPP treatment IP (n = 3 per group). Whole colon tissue was collected and processed for RNA-seq analysis. (A) Heat map representation of log<sub>2</sub> transformed readcount data for significant differentially expressed genes with a log<sub>2</sub> fold change >1. (B) Analysis of mRNA expression for validation of RNA-seq results using qPCR of processed whole colon tissue samples. (C) Representative fluorescent microscopy images (200x total magnification) of embedded mouse colon tissue from WT mice 24h after receiving PBS or CoPP IP. (D) Representative fluorescent microscopy image (200x magnification) of mouse colon stained for F4/80 and HO-1, 24h after receiving CoPP. (E-H) WT mice were treated with PBS or CoPP

and CD11b<sup>+</sup>CX3CR1<sup>+</sup>CD64<sup>+</sup>MHCII<sup>+</sup>Ly6C<sup>-</sup> colonic macrophages were recovered after two days. Results reflect combined data from three independent experiments, each with 3–5 pooled mice per group. (E) Percentage median fluorescence intensity (MFI) values of MHC class II staining on colonic macrophages isolated from WT PBS vs CoPP treated mice. (F) Gene expression of erythrophagocytic markers from intestinal macrophages isolated from WT PBS vs CoPP treated mice. (H) Inflammatory gene expression from colonic macrophages recovered from individual WT mice treated with PBS vs CoPP and analyzed at baseline or 2h after LPS treatment (n = 3 for controls and 4 – 6 for LPS treated). \* $p < .05$ , \*\* $p < .01$ , \*\*\* $p < .001$ .

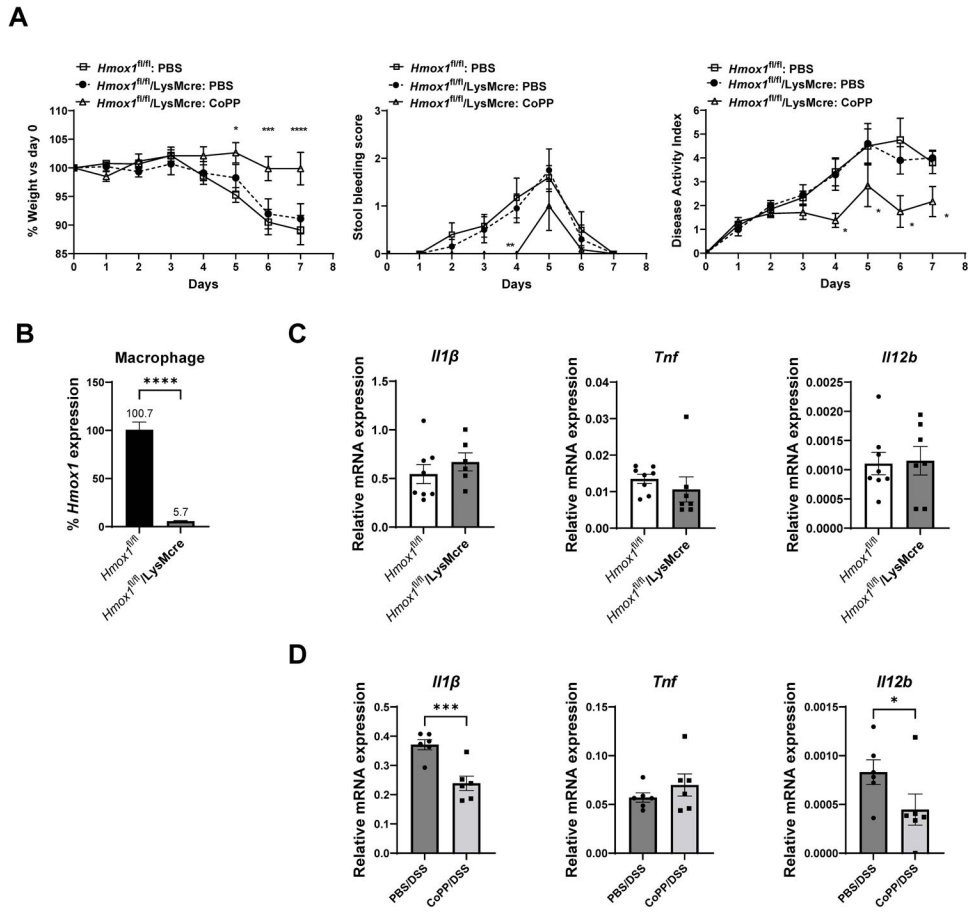


**Figure 3. Protective influence of CoPP is independent of macrophage HO-1.**

(A) Percent weight loss, stool bleeding scores and combined disease activity index after 7 days from *Hmox1<sup>fl/fl</sup>* and *Hmox1<sup>fl/fl</sup>/LysMcre* mice that received 2.5% DSS in drinking water x 5 days, and were treated with vehicle or CoPP IP (n = 5 – 6 per group and are representative of two or more independent experiments). (B-C) At day 5 of a DSS colitis experiment CD11b<sup>+</sup>CX3CR1<sup>+</sup>CD64<sup>+</sup>MHCII<sup>+</sup>Ly6C<sup>-</sup> colonic macrophages were isolated from *Hmox1<sup>fl/fl</sup>* and *Hmox1<sup>fl/fl</sup>/LysMcre* mice (n = 4 – 5 per group) using FACS. (B) Gene expression was evaluated for *Hmox1*, which is normalized to *Hmox1<sup>fl/fl</sup>* mouse macrophage expression levels. (C) Relative mRNA expression of inflammatory cytokines from isolated colonic macrophages. Results reflect combined data from two independent experiments. (D) Gene expression evaluated in colonic macrophages isolated from vehicle or CoPP treated WT mice at day 5 of a 3% DSS experiment. \**p* < .05, \*\**p* < .01, \*\*\**p* < .001, \*\*\*\**p* < .0001 (in panel A, the comparisons are between the two *Hmox1<sup>fl/fl</sup>/LysMcre* groups).

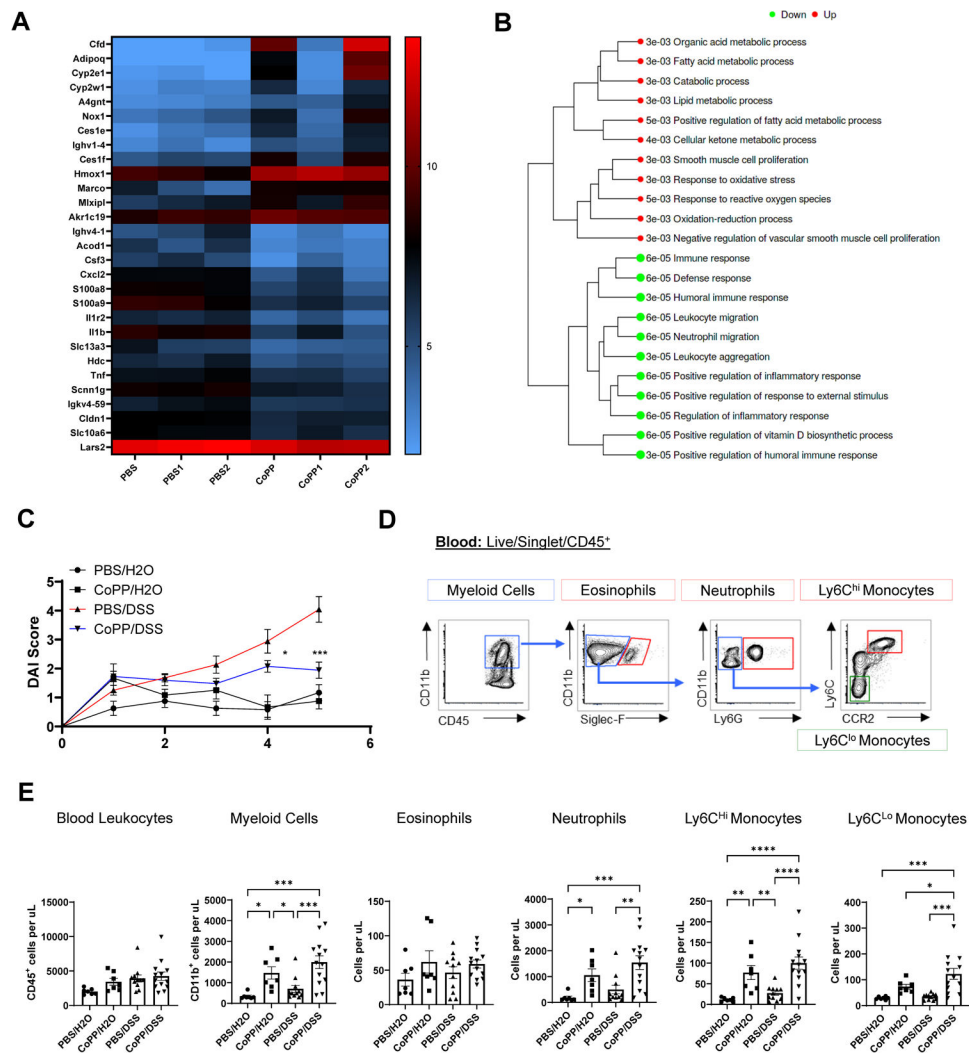


**Figure 4. CoPP influences leukocyte mobilization during inflammation.**

Colon tissue was collected and processed for RNA-seq analysis from WT mice that received 2.5% DSS in drinking water for 5 days along with either PBS or CoPP treatment IP ( $n = 3$  per group). (A) Heat map representation of log<sub>2</sub> transformed readcount data for significant differentially expressed genes with a log<sub>2</sub> fold change >1. (B) Enrichment analysis for DEGs using GO biological process approach. (C) Combined disease activity index (DAI) from WT mice that received water, or 2.5% DSS in their drinking water, for 5 days and were treated with PBS or CoPP IP ( $n = 8 - 13$  per group). Combined results from 3 independent experiments ( $*p < .05$ ,  $***p < .001$  reflecting PBS/DSS vs CoPP/DSS comparison). (D) Blood leukocytes were isolated and quantified using flow cytometry by assessing for CD45, Ly6G, Siglec-F, CD11b, Ly6C and CCR2 expression with representative contour plots of live/singlet/CD45<sup>+</sup> cells shown. (E) Cell counts of blood leukocyte populations represented as cells per  $\mu$ L. Combined results from 3 independent experiments ( $n = 8 - 13$  per group).  $*p < .05$ ,  $**p < .01$ ,  $***p < .001$ ,  $****p < .0001$ .

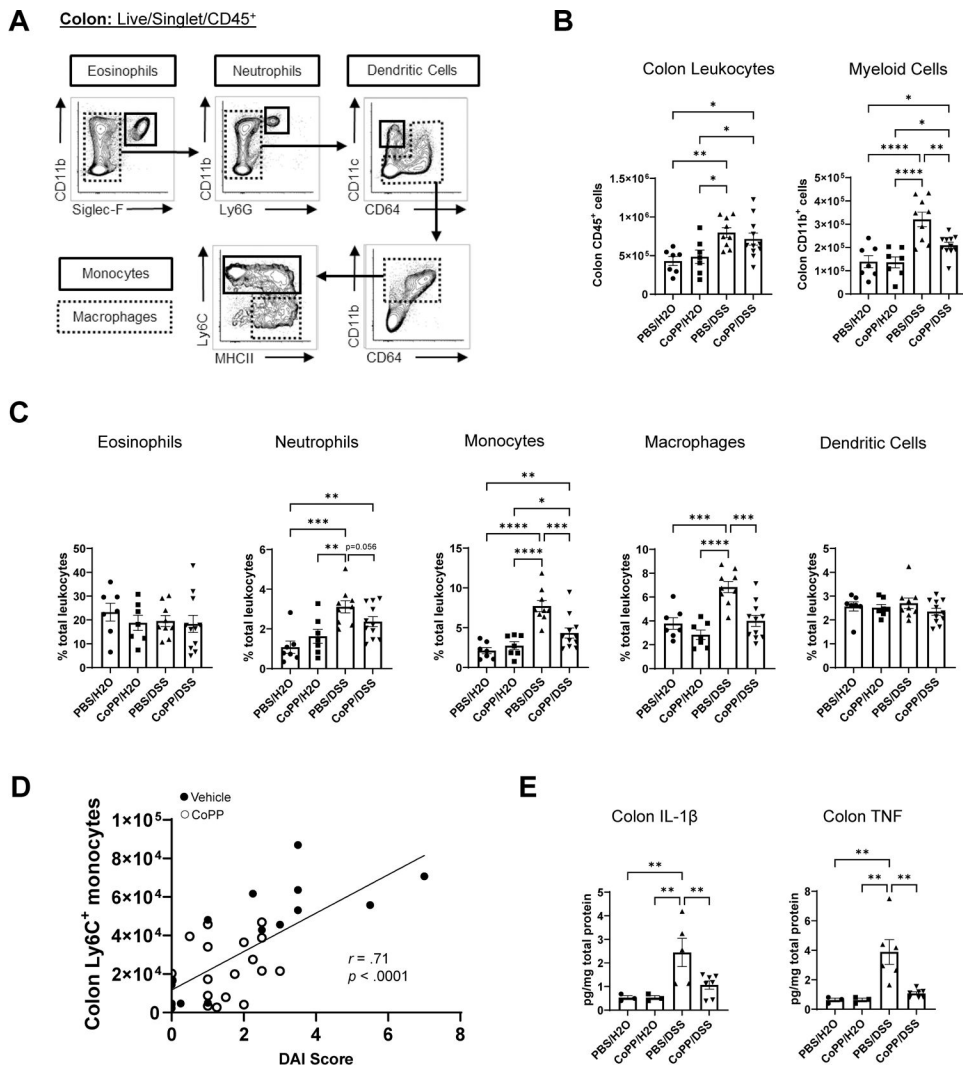


**Figure 5. Contradictory colonic myeloid trafficking in response to CoPP.** Colon tissue was isolated from WT mice receiving water or DSS for 5 days along with IP PBS or CoPP. (A) Colon lamina propria cells were isolated and assessed for the expression of CD45, Ly6G, Siglec-F, CD11b, Ly6C, CD64, CD11c and MHCII with representative flow cytometry contour plots of live/singlet/CD45<sup>+</sup> cells shown. (B) Cell counts of colon total leukocytes and myeloid cells based on CD45 and CD11b staining. (C) Proportion of colon leukocyte populations as a percentage of total CD45<sup>+</sup> cells. (D) Pearson correlation of colonic monocyte population compared with disease activity index (PBS treated, black; CoPP treated, white). (E) Colonic concentration of inflammatory cytokines on a per mg total protein basis. \**p* < .05, \*\**p* < .01, \*\*\**p* < .001, \*\*\*\**p* < .0001.

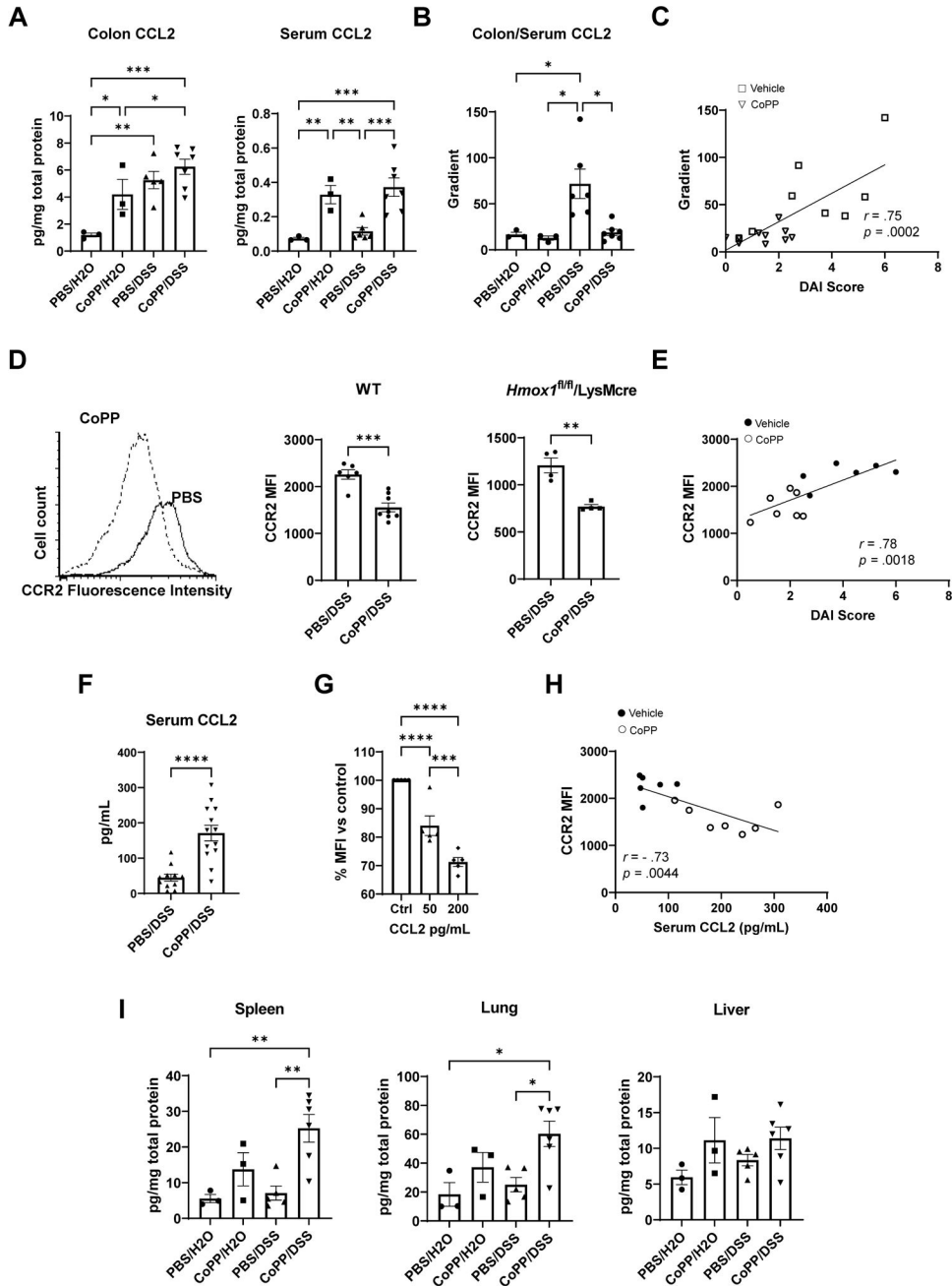


**Figure 6. CoPP elicits anti-inflammatory CCL2-CCR2 signaling in the setting of colitis.** WT mice received water or 2.5% DSS in their drinking water for 5 days and were treated with PBS or CoPP IP (n = 3 – 7 per group). (A) Whole colon tissue and blood serum was recovered and concentration of CCL2 was measured using ELISA detection, and presented as normalized to per mg total protein. (B) CCL2 concentration gradient strength calculated as chemokine level in the colon (per mg total protein) divided by corresponding serum level (per mg total protein). (C) Pearson correlation of CCL2 gradient strength compared to DAI score. (D) Representative flow cytometry histogram (WT mice) and median fluorescence intensity (MFI) values of CCR2 staining in Ly6C<sup>hi</sup> blood monocytes isolated at day 5 of

a DSS colitis experiment from WT and *Hmox1<sup>fl/fl</sup>*/LysMcre mice treated with vehicle or CoPP. (E) Pearson correlation of CCR2 MFI readings compared to DAI score from WT colitic mice treated with vehicle or CoPP at day 5. (F) Serum CCL2 concentration from WT colitic mice treated with PBS or CoPP at day 5 (n = 12 – 13 per group). (G) CCR2 MFI of blood Ly6C<sup>hi</sup> monocytes exposed ex-vivo to recombinant CCL2 for 1 hour, normalized to vehicle exposed monocytes. (H) Pearson correlation of CCR2 MFI from WT mouse blood Ly6C<sup>hi</sup> monocytes compared to serum CCL2 concentration from day 5 of a colitis experiment. (I) Segments of WT mouse spleen, lung and liver isolated and processed for CCL2 ELISA at day 5 of a DSS colitis experiment, presented as normalized to per mg total protein. Representative of duplicate experiments with similar results. \* $p < .05$ , \*\* $p < .01$ , \*\*\* $p < .001$ , \*\*\*\* $p < .0001$ .